

# ELECTRON CYCLOTRON HEATING MODELLING IN TOKAMAKS WITH 3D FULL WAVE CODE

V.Vdovin

RRC Kurchatov Institute, Nuclear Fusion Institute

We present modelling results of basic Electron Cyclotron Heating scenarios in tokamaks performed with newly developed 3D full wave STELEC (stellarator\_ECH, tokamaks included as particular case) code [1]. Code includes all basic wave physics as interference, diffraction, wave tunnelling, mode conversion at Upper Hybrid resonance to electron Bernstein waves and appropriate boundary conditions. Code operates in real 3D magnetic geometry and uses massive parallel terabyte computers and firstly permitted solution of above problem. The Upper Hybrid resonance plays important role, leading to strong broadening of power deposition profiles at fundamental harmonic with O-mode RF power launch. This is partly supported by experiments on DIII-D, RTP, T-10 and JT-60U. Diffraction effects are investigated at second harmonic and these are shown to be important even at moderate plasma densities. The O-X-B scheme for over dense plasma is also explored.

## 1. FTU and DIII-D Tokamaks Fundamental Harmonic Modeling

FTU tokamak with major radius  $R=93$  cm uses quasi perpendicular O-mode outside launch at 140 GHz. Contour plots of total wave electrical field are displayed in Fig.1a. The axis magnetic field  $B_0=4.667$  T, plasma density  $4.5 \times 10^{19} \text{ m}^{-3}$  (parabolic density profile,  $\alpha_n=1$ ),  $T_e(0)=9.2$  kV ( $\alpha_T=2$ ),  $I_p=0.72$  MA,  $N_{//}(0)=0.027$ . Upper Hybrid resonance  $\omega^2 = \omega_{ce}^2 + \omega_{pe}^2$  layer manifests itself, contrary to ray tracing, by bright “mirror” broadly radiating Electron Bernstein Waves (EBW)

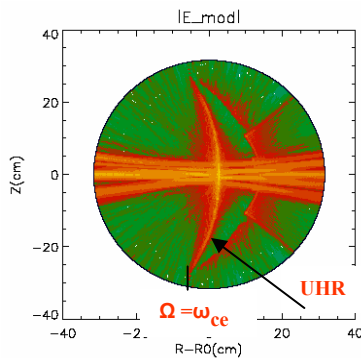


FIG.1a  $|E|_{total}$  in FTU at  $N_e=4.5 \times 10^{19} \text{ m}^{-3}$

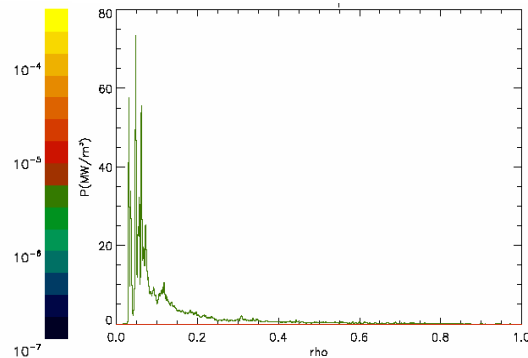


FIG.1b Power deposition  $P_e(\rho)$

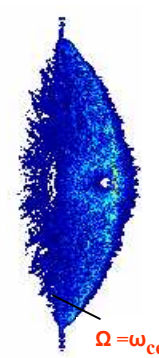


FIG.1c 2D  $P_e$

and slow X-waves to cold ECR side. Averaged over flux surface power deposition, in Fig.1b, shows peaked power deposition mainly responding to large electrical fields near UHR layer ( $X=3$  cm). This is confirmed by 2D power deposition in Fig.1c. Thus RF power is absorbed far away from cold EC resonance ( $X=-6$ cm). This ECH picture summarizes early record ECH results from middle and small tokamaks T-10, TFR, RTP etc. obtained at low plasma densities ( $\sim 10^{19} \text{ m}^{-3}$ ) when distance between ECR and UHR resonances  $\Delta X \sim R n(0)$  is small one.

Contour plots of  $|E\_minus|$  wave electrical field in DIII-D plasma are displayed in Fig.2a at fundamental harmonic O-mode 44.6 GHz launch:  $N_{||}(0) = 0.227$ ,  $N_e(0) = 0.48 \times 10^{19} \text{ m}^{-3}$ ,  $N_{es} = 0.12 \times 10^{19} \text{ m}^{-3}$ ,  $T_e(0) = 2.7 \text{ kV}$  ( $\alpha_n = 0.2$ ,  $\alpha_T = 2$ ),  $B_0 = 1.47 \text{ T}$ ,  $I_p = 0.657 \text{ MA}$ . plasma elongation is  $\kappa = 1.65$ , triangularity  $\delta = 0.5$ . The EC resonance is far inside displaced one. Power deposition peaks in Fig.2b may be responsible for temperature filamentation. The benefits off centre inside EC resonance scenario are supported by T-10 experience (K.Razumova).

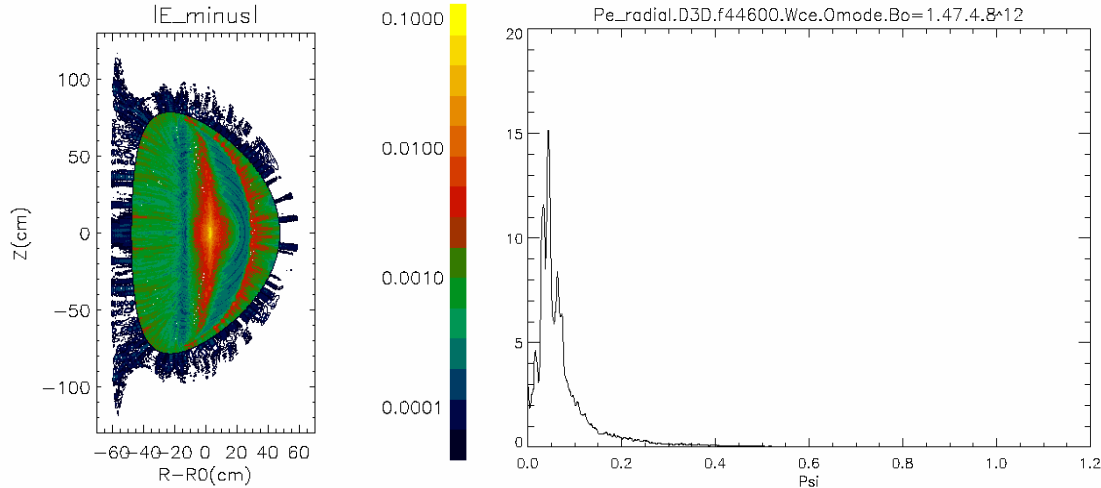


FIG.2a  $|E\_minus|$  in DIII-D

FIG.2b  $P_e(\rho)$  in DIII-D at  $N_{||}(0) = 0.227$

Again, power deposition is dominated by UH resonance position due to large amplitudes of converted waves. One pays attention that RF power is absorbed by fast electrons.

## 2. Second Harmonic ECH Scenarios in T-10

Majority of present tokamaks and stellarators operate at second harmonic and at for not so large plasma densities UHR is absent one. Second harmonic X-mode launch in T-10:  $|real(E\_psi)|$ , Fig.3a at  $N=90$  ( $N_{||}(0) = 0.02$ ),  $F = 140 \text{ GHz}$   $N_e(0) = 4.5 \times 10^{19} \text{ m}^{-3}$ ,  $T_e(0) = 8.7 \text{ kV}$ , ( $\alpha_n = 1$ ,  $\alpha_T = 2$ ),  $B_0 = 2.5 \text{ T}$ ,  $I_p = 300 \text{ kA}$  (relativistic effects are included) and power deposition in Fig.3b.

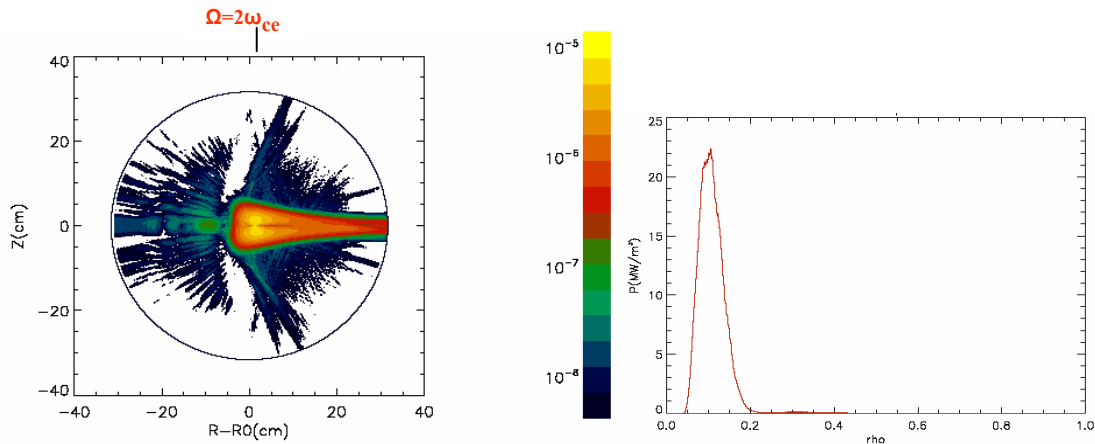


FIG.3a  $|real(E\_psi)|$  in T-10 at  $N_e(0) = 4.5 \times 10^{19} \text{ m}^{-3}$

FIG.3b  $P_e(\rho)$  in T-10 at  $2\omega_{ce} F = 140 \text{ GHz}$

At plasma density  $N_e(0)=9 \times 10^{19} \text{ m}^{-3}$  diffraction is more strong one (Figs.4a,b).

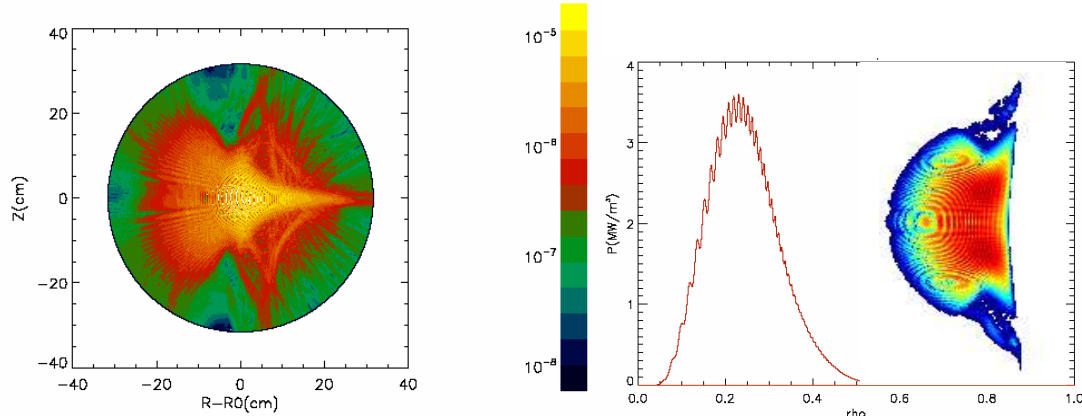


FIG.4a  $|real(E_{psi})|$  in T-10,  $N_e(0)=9 \times 10^{19} \text{ m}^{-3}$  FIG.4b 1D&2D  $P_e$  in T-10 at  $N_e=9 \times 10^{19} \text{ m}^{-3}$

### 3. Second Harmonic ECH Scenarios in DIII-D at Oblique Launch

Second harmonic X-mode oblique 4 MW launch in DIII-D: plasma elongation  $\kappa=1.65$ , triangularity  $\delta=0.5$ ,  $N=920$  ( $N/(0)=0.29$ ),  $F=89.2 \text{ GHz}$ ,  $T_e=7.2 \text{ kV}$ ,  $N_e(0)=1.2 \times 10^{19} \text{ m}^{-3}$ ,  $I_p=720 \text{ kA}$ ,  $q(0)=0.82$ ,  $q(a)=3.5$  is displayed in Figs.5a,b: by  $|real(E_{minus})|$  and  $|real(E_{psi})|$

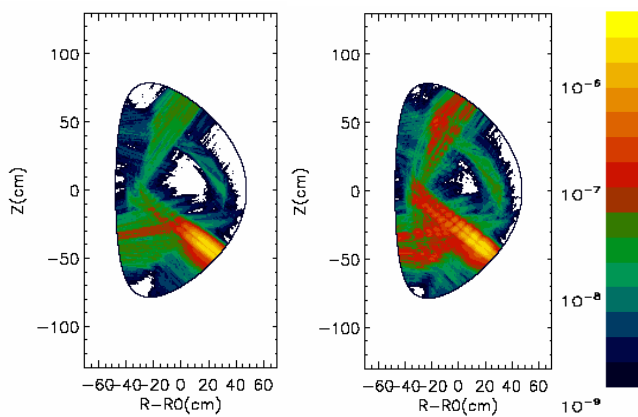


FIG.5a  $|real(E_{minus})|$  in DIII-D at  $2\omega_{ce}$  FIG.5b  $|real(E_{psi})|$  in DIII-D at  $2\omega_{ce}$

fields components. Radial power depositions calculated by STELEC and GENRAY-GA (R.Prater [2]) for elliptically polarized X antenna are given by Figs.5a,b. One can see that STELEC gives up to 3 times broader power deposition than predicts ray tracing code.

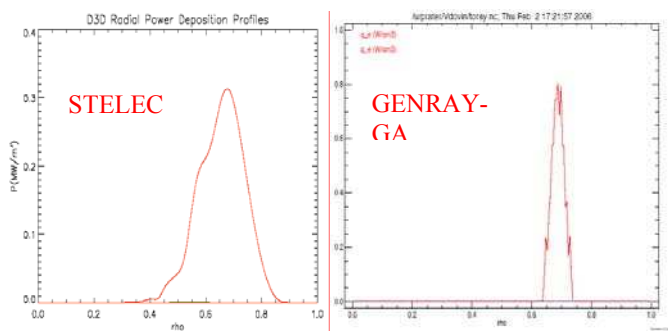
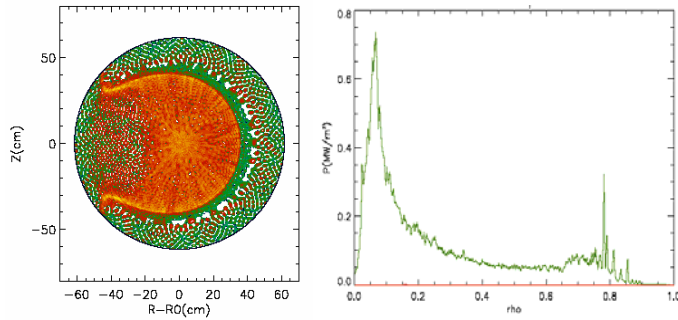


FIG.6a  $P_e(\rho)$  in DIII-D calculated by STELEC FIG.6b  $P_e(\rho)$  in DIII-D due to GENRAY-GA

### 5. OXB Scenarios For Over Dense Plasma

These schemes were theoretically proposed in frame of 1D geometry to exploit O-mode conversion to X-mode with subsequent its conversion to EB waves (O-X- B scheme) which have no

density cut off and can propagate at plasma densities larger than cut off densities for e.m. EC waves. We modeled this OXB scheme at fundamental harmonic in Tore Supra tokamak with



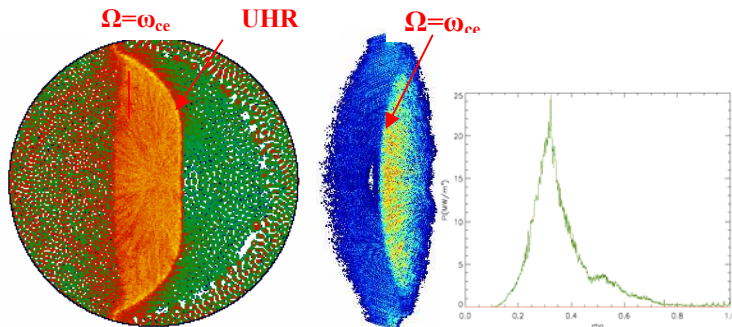
$R_0=2.38$  m,  $a=0.61$  m,  $N=80$   
 $(N_{//}(0)=0.125)$ ,  $F=12.85$  GHz,  $T_{e0} =$   
 $9.5$  kV,  $N_e(0) = 6 \times 10^{17}$  m $^{-3}$ , thus  
 $N_e(0) = 1.7 N_{crit}$ ,  $(\alpha_n=2.5, \alpha_T=0.1)$ ,  
 $B_0= 0.37$  T,  $I_p= 103$  kA,  $q(0)=1.35$ ,  
 $q(a)=3.65$ . STELEC code

FIG.7a  $|real(E_{\psi})|$  in Tore Supra      FIG.7b  $P_e(\rho)$  in TS at  $N_e(0) = 1.7 N_{crit}$

found that really O-X-B 2D scheme operates in regime with far inside EC resonance location as demonstrated by Fig.7a for  $|real(E_{\psi})|$  contour plots and by Fig.7b for radial power deposition  $P_e(r)$ . However we did not succeed at second harmonic O-mode launch in DIII-D and Tore Supra. More work is needed.

### 6. Fundamental harmonic ECH power deposition in RTP

The RTP tokamak (major radius  $R=72$  cm) [3] used oblique O-mode fundamental harmonic outside launch at 60 GHz in Co-Counter ECCD scenarios. Contour plots of  $|real(E_{\psi})|$  wave electrical field, 2D and 1D power depositions are displayed in Fig.8. The axis magnetic field is  $B_0=1.98$  T, central plasma density  $1.65 \times 10^{19}$  m $^{-3}$  (parabolic density profile),  $T_e(0)=2.9$  kV ( $\alpha_T=2$ ),  $I_p=40$  kA,  $N_{//}(0)=0.35$ . One sees that EB waves play crucial role in creation of EC power deposition profile. Classical Doppler effects. Counter CD scenario with  $N_{//}(0)=-0.35$  reveals



significant amount of RF power being deposited broadly near half of plasma minor radius, consistent with reduced counter CD efficiencies in RTP.

FIG.8  $|real(E_{\psi})|$  and Power depositions: 1D  $P_e(\rho)$  and 2D  $P_e(\rho, \theta)$  in RTP

### Conclusions

In toroidal bounded plasmas O-mode and X-mode are coupled ones through space inhomogeneity and boundary conditions. This modes coupling effect in toroidal plasmas is especially strong one at fundamental harmonic scenarios due to singular layer created by UHR resonance. This UHR effect leads to strong broadening of EC power deposition at fundamental and must be accounted through full wave codes. In second harmonic scenarios modes coupling is more weak one. Ray tracing/bi-tracing technique may be still used.

### References

1. V.Vdovin *Electron Cyclotron Heating modelling in tokamaks with full wave 3D code, 14th Joint Workshop on ECH and ECE, 9- 12 May 2006, Santorini island, Greece*
2. R. Prater (private communication).
3. A.Donne, A.Oomens, Proc. EC-9 (1995), 645, F.Schuller et al., Proc. of 4<sup>th</sup> SMP (1999)